

Out-of-equilibrium versus dynamical and thermodynamical transitions for a model protein

Alberto IMPARATO¹, Stefano LUCCIOLI^{2,3}, Alessandro TORCINI^{2,3}

(1) *Dept. of Physics and Astronomy, University of Aarhus, Ny Munkegade, Building 1520 - DK-8000 Aarhus C, Denmark*

(2) *Istituto dei Sistemi Complessi, CNR, via Madonna del Piano 10, I-50019 Sesto Fiorentino, Italy*

(3) *INFN, Sez. Firenze, and CSDC, via Sansone, 1 - I-50019 Sesto Fiorentino, Italy*

Equilibrium and out-of-equilibrium transitions of an off-lattice protein model have been identified and studied. In particular, the out-of-equilibrium dynamics of the protein undergoing mechanical unfolding is investigated, and by using a work fluctuation relation, the system free energy landscape is evaluated. Three different structural transitions are identified along the unfolding pathways. Furthermore, the reconstruction of the free and potential energy profiles in terms of inherent structure formalism allows us to put in direct correspondence these transitions with the equilibrium thermal transitions relevant for protein folding/unfolding. Through the study of the fluctuations of the protein structure at different temperatures, we identify the dynamical transitions, related to configurational rearrangements of the protein, which are precursors of the thermal transitions.

Subject Index: 02, 07,55

§1. Introduction

Biopolymers such as proteins and nucleic acids are paradigmatic examples of complex systems. Similarly to glasses and to super-cooled liquids, they are characterized by complex free energy landscapes (FELs), which determine their dynamical and thermodynamical properties. Manipulation experiments on single biomolecules have made it possible to observe unfolding and refolding trajectories of single proteins,¹⁾ or RNA molecules.^{2),3)} From a theoretical point of view, the unfolding and refolding of biomolecules represent typical stochastic processes where out-of-equilibrium single trajectories of microscopic systems can be observed, since the typical experimental time is much smaller than the typical molecular relaxation time. When a thermodynamical system is driven far from equilibrium, classical linear response theories and other near-equilibrium approximations generally fail. However, in recent years some general relations for systems driven far from equilibrium by large external perturbation have been obtained. These relations, which are known as fluctuation relations,⁴⁾ go beyond linear response theory valid only in the vicinity of the equilibrium regime. On the one hand, single molecule experiments represent excellent test-bed for these results obtained in the field of out-of-equilibrium statistical mechanics.³⁾ On the other hand, these relations can be used to characterize the thermodynamical properties of biomolecules, overcoming the intrinsic out-of-equilibrium nature of the unfolding experiments. In particular, a fluctuation relation introduced by Hummer and Szabo⁵⁾ can be used to estimate the equilibrium free energy land-

scape of a system as a function of an internal coordinate: such a relation has been used to evaluate the FEL of model^(6)–8) as well as of real proteins.^{9),10)}

In two previous papers,⁷⁾ we have shown that the free energy landscape of a model protein can also be evaluated by using the inherent structure (IS) approach, a method previously used to characterize the structural-arrest temperature in glasses¹¹⁾ and super-cooled liquids.¹²⁾ The investigation of the IS distributions allows us to give an estimate of the energetic barriers separating the native state from the completely stretched configuration along the out-of-equilibrium unfolding trajectories. Moreover, the thermal energies to overcome these barriers are related to three temperatures, which are quite similar to the temperatures usually employed to characterize the thermodynamical transitions associated to protein folding.

Thus, the aim of this paper, is twofold. On the one hand we want to reconstruct via out-of-equilibrium measurements the free energy landscape of a model protein, by using both a fluctuation relation and IS approach. On the other hand, we want to characterize the equilibrium dynamical transitions for the same model protein induced by temperature variation, and to compare these with the information gathered via the out-of-equilibrium mechanical manipulations.

The paper is organized as follows, in Section 2 we briefly describe the model protein used in the present work, and the numerical simulations we perform. In Section 3, we introduce the work fluctuation relation and reconstruct the free energy landscape by combining it with out-of-equilibrium unfolding simulations. We discuss how the FEL can be evaluated via the IS approach in Section 4, and make a comparison with the results obtained in the previous Section 3. In Section 5, we discuss the three characteristic temperatures characterizing the thermal unfolding of the protein, and relate them to the structural transition as identified in the Sect. 4. Section 6 is devoted to the analysis of the dynamical transitions observed for this model protein, which appear to be precursors of the thermal unfolding transitions. We conclude and summarize our results in Sect. 7.

§2. The protein model

The model studied in this paper is a modified version of the 3d off-lattice model introduced by Honeycutt-Thirumalai¹³⁾ and successively generalized by Berry *et al.* to include a harmonic interaction between next-neighboring beads instead of rigid bonds.¹⁴⁾ The model consists of a chain of L point-like monomers mimicking the residues of a polypeptidic chain. For the sake of simplicity, only three types of residues are considered: hydrophobic (B), polar (P) and neutral (N) ones.

The intramolecular potential is composed of four terms: a nearest-neighbor harmonic potential, V_1 , intended to maintain the bond distance almost constant, a three-body interaction V_2 , which accounts for the energy associated to bond angles, a four-body interaction V_3 corresponding to the dihedral angle potential, and a long-range Lennard-Jones (LJ) term, V_4 , acting on all pairs i, j such that $|i - j| > 2$, namely

$$V_1(r_{i,i+1}) = \alpha(r_{i,i+1} - r_0)^2, \quad (2.1)$$

$$V_2(\theta_i) = A \cos(\theta_i) + B \cos(2\theta_i) - V_0, \quad (2.2)$$

$$V_3(\varphi_i, \theta_i, \theta_{i+1}) = C_i[1 - S(\theta_i, \theta_{i+1}) \cos(\varphi_i)] + D_i[1 - S(\theta_i, \theta_{i+1}) \cos(3\varphi_i)], \quad (2.3)$$

$$V_4(r_{i,j}) = \varepsilon_{i,j} \left(\frac{1}{r_{i,j}^{12}} - \frac{c_{i,j}}{r_{i,j}^6} \right). \quad (2.4)$$

Here, $r_{i,j}$ is the distance between the i -th and the j -th monomer, θ_i and φ_i are the bond and dihedral angles at the i -th monomer, respectively. The parameters $\alpha = 50$ and $r_0 = 1$ fix the strength of the harmonic force and the equilibrium distance between successive monomers. Both α and r_0 , as well as all the quantities in the following are expressed in dimensionless units, for a comparison with physical units see.¹⁵⁾

The value of α is chosen to ensure a value for V_1 much larger than the other terms of potential in order to reproduce the stiffness of the protein backbone. The expression for the bond-angle potential term $V_2(\theta_i)$ (2.2) corresponds, up to the second order, to a harmonic term $\sim k_\theta(\theta_i - \theta_0)^2/2$, where

$$A = -k_\theta \frac{\cos(\theta_0)}{\sin^2(\theta_0)}, \quad B = \frac{k_\theta}{4 \sin^2(\theta_0)}, \quad V_0 = A \cos(\theta_0) + B \cos(2\theta_0) \quad , \quad (2.5)$$

with $k_\theta = 20$ and $\theta_0 = 5\pi/12$ rad or 75° .

The dihedral angle potential is characterized by three minima for $\varphi = 0$ (associated to a so-called *trans state*) and $\varphi = \pm 2\pi/3$ (corresponding to *gauche states*), this potential is mainly responsible for the formation of secondary structures. In particular large values of the parameters C_i, D_i favor the formation of trans state and therefore of β -sheets, while when gauche states prevail α -helices are formed. The parameters (C_i, D_i) have been chosen in the following way: if two or more beads among the four defining φ are neutral (N) then $C_i = 0$ and $D_i = 0.2$; in all the other cases $C_i = D_i = 1.2$. The *tapering function* $S(\theta_i, \theta_{i+1})$ has been introduced in the expression of V_3 in order to cure a well known problem in the dihedral potentials, for more details see.^{7),16)} The quantity $S(\theta_i, \theta_{i+1})$ entering in the definition of V_3 has a limited influence on the dynamics apart in proximity of some extreme cases.

The last term V_4 , introduced to mimic effectively the interactions with the solvent, is a Lennard-Jones potential, which depends on the type of interacting residues as follows: if any of the two monomers is neutral the potential is repulsive $c_{N,X} = 0$ and its scale of energy is fixed by $\varepsilon_{N,X} = 4$; for interactions between hydrophobic residues $c_{B,B} = 1$ and $\varepsilon_{B,B} = 4$; for any polar-polar or polar-hydrophobic interaction $c_{P,P} \equiv c_{P,B} = -1$ and $\varepsilon_{P,P} \equiv \varepsilon_{P,B} = 8/3$.

Accordingly, the Hamiltonian of the system reads

$$H = K + V = \sum_{i=1}^L \frac{p_{x,i}^2 + p_{y,i}^2 + p_{z,i}^2}{2} + \sum_{i=1}^{L-1} V_1(r_{i,i+1}) + \sum_{i=2}^{L-1} V_2(\theta_i) + \sum_{i=2}^{L-2} V_3(\varphi_i, \theta_i, \theta_{i+1}) + \sum_{i=1}^{L-3} \sum_{j=i+3}^L V_4(r_{ij}) \quad (2.6)$$

where all monomers are assumed to have the same unitary mass, and consequently the momenta can be defined as $(p_{x,i}, p_{y,i}, p_{z,i}) \equiv (\dot{x}_i, \dot{y}_i, \dot{z}_i)$.

In the present paper we consider the following sequence of 46 monomers:

$$B_9N_3(PB)_4N_3B_9N_3(PB)_5P$$

This sequence that has been widely analyzed in the past for thermal folding^{13)–15), 17)–21)} as well as for mechanically induced unfolding and refolding.^{7), 22), 23)} The sequence studied exhibits a four stranded β -barrel Native Configuration (NC), which is stabilized by the attractive hydrophobic interactions among the B residues (see configuration (a) in Fig. 3). In particular the first and third B_9 strands, forming the core of the NC, are parallel to each other and anti-parallel to the second and fourth strand, namely, $(PB)_4$ and $(PB)_5P$. These latter strands are instead exposed towards the exterior due to the presence of polar residues.

In the following we will report simulation results associated to two different kind of simulation protocols: equilibrium molecular dynamics (MD) canonical simulations at temperature T performed by integrating the corresponding Langevin equation; steered out-of-equilibrium MD simulations intended to mimic the mechanical pulling at constant velocity of a protein attached to the cantilever of an atomic force microscope, or analogously when trapped in optical tweezers. In both cases the initial state of the system is taken equal to the native configuration (NC), that we assume to coincide with the minimal energy configuration.

§3. Fluctuation relation and out-of-equilibrium unfolding

Given a system with L particles, characterized by the Hamiltonian $H_0(q)$, where $q = \{\mathbf{r}_i, \mathbf{p}_i\}$ is a point in the system phase space, we are interested in evaluating the constrained free energy landscape

$$\beta f_J(Q) \equiv -\ln \left[\int dq \delta(Q - Q(q)) e^{-\beta H_0(q)} \right], \quad (3.1)$$

where Q is some macroscopic observable, function of the microscopic coordinates q . If the system is driven out of equilibrium by an external potential $U_{z(t)}(Q)$, which depends explicitly on Q and on the external parameter z , whose temporal evolution is dictated by the protocol $z = z(t)$, then the FEL (3.1) can be obtained via the work fluctuation relation⁵⁾

$$\left\langle \delta(Q - Q(q)) e^{-\beta W} \right\rangle = e^{-\beta [f_J(Q) + U_{z(t)}(Q)]} / Z_0 \quad . \quad (3.2)$$

In Eq. (3.2) W is the work exerted on the system by the force associated with the potential U , and the symbol $\langle \cdot \rangle$ refers to an average over all the possible stochastic trajectories spanning the system phase space, while the parameter $z(t)$ changes over time. Z_0 is the partition function associated with the unperturbed Hamiltonian $H_0(q)$.

Typically, the macroscopic observable characterizing the state of a biopolymer under mechanical stress is the end-to-end distance ζ and this is the coordinate we will

consider in the following. Furthermore, we consider a quadratic potential $U_{z(t)}(\zeta) = k/2(\zeta - z(t))^2$, mimicking the effect of the force exerted on the molecule by the cantilever of an atomic force microscope, or by optical tweezers, where $z(t) = v_p \times t$, is the equilibrium position of the potential, moving with a constant velocity v_p . We perform steered MD unfolding simulations, where one of the free ends of the molecules is kept fixed, while the other is pulled by the external force $k(\zeta(t) - z(t))$ associated with the potential U . Further details on the simulations are given in Ref.⁷⁾ We consider different values of v_p , and for each of them we simulate a given number of unfolding trajectories. For each trajectory, we compute the work W done by the external force on the protein. Finally, in order to estimate $f_J(\zeta)$ from Eq. (3.2) we use the procedure introduced and discussed in Ref.²⁴⁾ The results are plotted in Fig. 1 for different pulling velocities v_p : we notice that as the velocity v_p decreases, the curves collapse onto the same curve which corresponds to the best estimate of $f_J(\zeta)$ given by the method described here. In Ref.⁷⁾ we have verified that the lower curve essentially coincides with an independent equilibrium estimate of the FEL obtained via the weighted histogram analysis method.

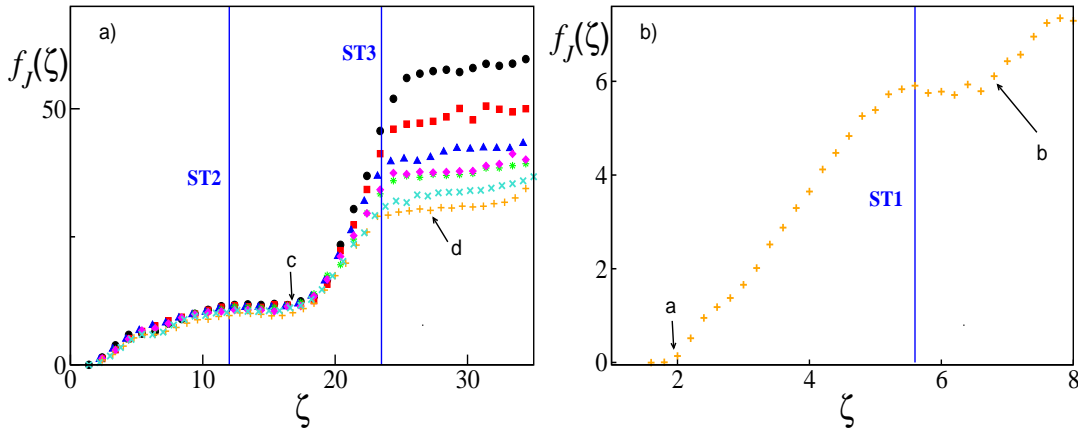


Fig. 1. Free-energy profiles f_J as a function of the end-to-end distance ζ , for the model protein discussed in Sec. 2, as obtained by implementing Eq. (3.2), with $T = 0.3$, and for different pulling velocities: from top to bottom $v_p = 5 \times 10^{-2}$, 1×10^{-2} , 5×10^{-3} , 5×10^{-4} , 2×10^{-4} , 2×10^{-5} and 5×10^{-6} . In (b) an enlargement of the curve for $v_p = 5 \times 10^{-6}$ at small ζ is reported. The number of different pulling trajectories considered to estimate the profiles ranges between 150 and 250 at the highest velocities to 28 at the lowest velocity $v_p = 5 \times 10^{-6}$. The letters (a, b, c, d) indicate the value of $f_J(\zeta)$ corresponding to typical configurations reported in Fig. 3 and the (blue) vertical solid lines the location of the Structural Transitions (STs), see discussion in Sec. 4.

§4. Inherent structure formalism and structural transitions

Inherent structures correspond to local minima of the potential energy, in particular the phase space visited by the protein during its dynamical evolution can be decomposed into disjoint attraction basins, each corresponding to a distinct IS. Therefore, the canonical partition function can be expressed, within the IS formal-

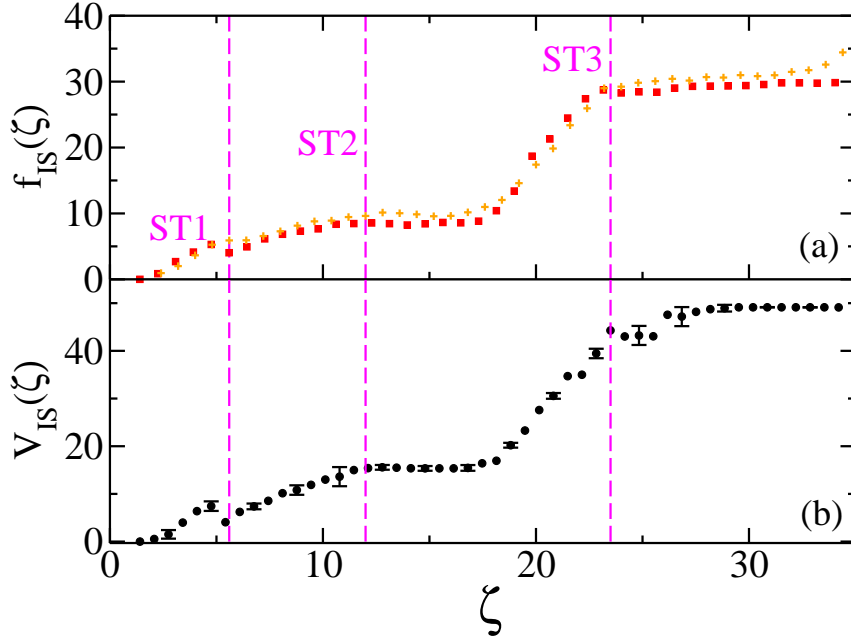


Fig. 2. (Color online) (a) Free energy profile $f_{IS}(\zeta)$ as a function of the end-to-end distance, (b) average potential energy $V_{IS}(\zeta)$ vs ζ . The dashed vertical lines indicate the location of the three structural transitions. All the data refer to a data bank of ISs obtained via out-of-equilibrium steered MD simulations mimicking mechanical protein unfolding performed at $T = 0.3$ with $v_p = 5 \times 10^{-4}$. In the upper panel (a) it is reported for comparison also $f_J(\zeta)$ (orange pluses) obtained via the fluctuation relation procedure with $v_p = 5 \times 10^{-6}$.

ism, as a sum over the non-overlapping basins of attraction, each associated to a specific minimum (IS) a :^{25)–27)}

$$Z_{IS}(T) = \frac{1}{\lambda^{3N'}} \sum_a e^{-\beta V_a} \int_{\Gamma_a} e^{-\beta \Delta V_a(\Gamma)} d\Gamma = \sum_a e^{-\beta [V_a + R_a(T)]} \quad (4.1)$$

where N' is the number of degrees of freedom of the system, λ is the thermal wavelength, Γ represents one of the possible conformations of the protein within the basin of attraction of a , V_a is the potential energy associated to the minimum a , $\Delta V_a(\Gamma) = V(\Gamma) - V_a$ and $R_a(T)$ the vibrational free energy due to the fluctuations around the minimum.

The free energy of the whole system at equilibrium is simply given by $f_{IS}(T) = -T \ln[Z_{IS}(T)]$. However, in order to construct a free energy landscape as a function of a parameter characterizing the different IS, like e.g. the end-to-end distance ζ , it is necessary to define a partition function restricted to ISs with an end-to-end distance within a narrow interval $[\zeta; \zeta + d\zeta]$

$$Z_{IS}(\zeta, T) = \sum'_a e^{-\beta [V_a + R_a(T)]} \quad (4.2)$$

where the \sum' indicates that the sum is not over the whole ensemble of ISs $\{a\}$ but restricted. The free energy profile as a function of ζ can be obtained by the

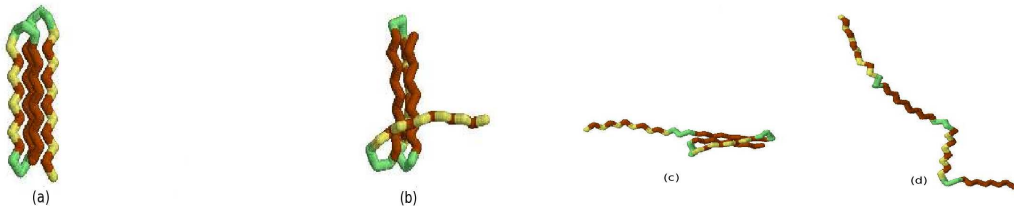


Fig. 3. (Color online) Typical configurations of the model protein along an unfolding trajectory driven by the mechanical force discussed in Section 3, with $T = 0.3$. The NC (a) has $\zeta_0 \sim 1.9$; the other configurations are characterized by $\zeta = 6.8$ (b), $\zeta = 16.8$ (c), and $\zeta = 27.1$ (d). The beads of type N , B , and P are colored in green, red and yellow, respectively.

usual relationship $f_{IS}(\zeta, T) = -T \ln[Z_{IS}(\zeta, T)]$; while the average potential energy, corresponding to ISs characterized by a certain ζ , can be estimated as follows:

$$V_{IS}(\zeta, T) = \frac{\sum_a V_a e^{-\beta[V_a + R_a(T)]}}{Z_{IS}(\zeta, T)} . \quad (4.3)$$

In order to build a data bank containing the different ISs, we have performed mechanical unfolding simulations of the protein at different temperatures via steered Langevin MD integration schemes. The data bank contains 3,000 – 50,000 ISs depending on the examined temperature as detailed in Ref.⁷⁾ It is worth to notice that the ISs have been collected by following out-of-equilibrium trajectories induced by mechanical manipulation on the NC at a velocity $v_p = 5 \times 10^{-4}$. As shown in Fig. 2 (a), the free energy profile reconstructed with this approach is almost coincident with the best estimate of $f_J(\zeta)$. However, the fluctuation relation procedure, described in the previous Section, requires a pulling velocity which is two orders of magnitude smaller in order to obtain a reliable reconstruction.

Moreover, referring to Fig. 1 and Fig. 2 (a), it is possible to identify the structural transitions (STs) induced by the pulling experiment. As shown in Fig. 1 (b), the free energy profile exhibits a clear minimum in correspondence of the end-to-end distance of the NC (namely, $\zeta_0 \sim 1.9$). In more detail, up to $\zeta \sim 5.6$, the protein remains in native-like configurations characterized by a β -barrel made up of 4 strands, while the escape from the native valley is signaled by the small dip at $\zeta \sim 5.6$ and it is indicated as ST1 in Fig. 1 (b) and Fig. 2 (a).

For $\zeta > 6$ the configurations are characterized by an almost intact core (made of 3 strands) plus a stretched tail corresponding to the pulled fourth strand (see configuration (b) in Fig. 3). The second ST amounts to pull the strand $(PB)_5P$ out of the barrel leading to configurations similar to (c) reported in Fig. 3. In the range $13 < \zeta < 18.5$ the curve $f_{IS}(\zeta)$ appears as essentially flat, thus indicating that almost no work is needed to completely stretch the tail once detached from the barrel. The pulling of the third strand (that is part of the core of the NC) leads to a definitive destabilization of the β -barrel. This transition is denoted as ST3 in Fig. 2 (a). The second plateau in $f_{IS}(\zeta)$ corresponds to protein structures made up of a single elongated strand (an example of this state is configuration (d) in Fig. 3).

§5. Thermodynamical transition temperatures

The main thermodynamic features of a protein can be summarized with reference to three different transition temperatures:^{7),17),20),25),28)} the collapse temperature T_θ discriminating between phases dominated by random-coil configurations rather than collapsed ones; the folding temperature T_f , below which the protein stays predominantly in the native valley; and the glassy temperature T_g indicating the freezing of large conformational rearrangements.²⁷⁾ Following the procedures reported in Ref.,²⁸⁾ we have determined these temperatures and obtained $T_\theta = 0.65(1)$, $T_f = 0.255(5)$, and $T_g = 0.12(2)$. These values are in good agreement with those reported in,^{17),20)} where T_f and T_g have been identified via different protocols.

Then, we can try to put in correspondence the three unfolding stages previously discussed in Sec. 4 with thermodynamical aspects of the protein folding. In particular, by considering the energy profile $V_{IS}(\zeta)$ reported in Fig. 2 (b), an energy barrier ΔV_{IS} and a typical transition temperature $T_t = (2\Delta V_{IS})/(3N)$, can be associated to each of the STs. The first transition ST1 corresponds to a barrier $\Delta V_{IS} = 8(1)$ and therefore to $T_t = 0.11(1)$, that, within error bars, essentially coincide with T_g . For the ST2 transition to occur, the barrier to overcome is $\Delta V_{IS} = 16(1)$ and this is associated to a temperature $T_t = 0.23(2)$ (slightly smaller than T_f). The energetic cost to completely stretch the protein is $50(1)$ that corresponds to a transition temperature $T_t = 0.72(1)$, that is not too far from the θ -temperature given above. At least for this specific sequence, our results indicate that the observed out-of-equilibrium STs induced by mechanical pulling can be put in direct relationship with equilibrium thermal transitions usually characterizing the folding/unfolding processes.

§6. Dynamical transitions and structure fluctuations

In the analysis of equilibrium properties of heteropolymers, an abrupt deviation of the structural mean square displacement from a linear temperature dependence is usually associated to a *dynamical transition*.³⁰⁾ Fluctuations of the protein structure at equilibrium have been studied experimentally via elastic incoherent neutron scattering as well as Mössbauer absorption spectroscopy.^{30)–32)} These studies indicate the existence of different dynamical regimes separated by dynamical transitions,³⁰⁾ in particular for hydrated proteins powders, a first non-linear enhancement of the mean square displacement with the temperature is observed around 150 K, and a second one around 240 K. The first dynamical transition is associated to torsional motions and observable also for dehydrated or solvent-vitrified system, while the second one is related to the onset of small-scale libration motions of side-chains induced by water at the protein surface.

Fluctuations of the protein structure at a certain temperature can be characterized in terms of the following indicator²⁷⁾

$$\langle\langle \Delta u^2 \rangle\rangle = \frac{1}{L} \sum_{i=1}^L \Delta u_i^2 \quad \text{where} \quad \Delta u_i^2 = \langle d_{i,CM}^2 \rangle - \langle d_{i,CM} \rangle^2 \quad , \quad (6-1)$$

associated to the fluctuations of the distance $d_{i,CM}$ between the i -th residue and the center of mass of the protein, the symbols $\langle \cdot \rangle$ refer to temporal averages, while $\langle\langle \cdot \rangle\rangle$ to an average over all the beads composing the heteropolymer.

In the present case, we have estimated $\langle\langle \Delta u^2 \rangle\rangle$ for various temperatures T by performing equilibrium unfolding MD canonical simulations and by following the protein trajectory for a time $t = 500,000$. In Ref.²⁷⁾ the authors have shown for off-lattice G \bar{o} models, reproducing the B_1 domain of protein G, the existence of a dynamical transition temperature $T_D \sim 0.4 \times T_f$ denoting the onset of large scale fluctuations. As already mentioned in the previous Section, our model (as real proteins) is characterized by three different transition temperatures, at variance with the G \bar{o} model examined in Ref.²⁷⁾ where the folding and the collapse temperature coincide. It is therefore quite instructive to examine how many dynamical transitions are present in our model and their location in temperature.

From Fig. 4 (a) it is clear that $\langle\langle \Delta u^2 \rangle\rangle$ exhibits a linear behaviour until $T_{D1} \sim 0.2 \sim 0.78 \times T_f$ where a sharp increase takes place. At $T < T_{D1}$ the equilibrium dynamics is simply characterized by small harmonic oscillations of the beads around their equilibrium positions. Therefore by applying the theorem of equipartition of energy to the corresponding potential term (2.1) we expect that

$$\langle\langle \Delta u^2 \rangle\rangle = \frac{3}{2\alpha} \frac{L-1}{L} T = \gamma_1 T \quad \text{for } T \leq T_{D1} \quad , \quad (6.2)$$

as indeed verified (see Fig. 4(a)). By approaching the folding temperature there is a strong nonlinear enhancement of $\langle\langle \Delta u^2 \rangle\rangle$ due to a configurational rearrangement of the protein structure, which can be associated to an activation process which leads the protein to cross the free energy barrier at ST2 (see Fig. 2(a)).

Moreover just above T_f a second linear regime is observable. This is due to angular oscillations around their equilibrium positions θ_0 , therefore by applying equipartition to the terms V_1 and V_2 in our model we derive the following dependence

$$\langle\langle \Delta u^2 \rangle\rangle \sim \gamma_1 T + \frac{3}{k_\theta} \frac{L-2}{L} T = (\gamma_1 + \gamma_2) T \quad \text{for } T_f \leq T \leq T_{D2} \quad (6.3)$$

and again this linear behaviour is in good agreement with the data up to $T_{D2} \sim 0.5 \sim 0.77 \times T_\theta$ (see Fig. 4(a)). In this temperature range, the protein is partially unfolded, it is no more in native-like configurations, and the degrees of freedom associated to bending fluctuations, involving three consecutive beads, are now activated. At the temperature T_{D2} we observe a second dynamical transition involving large configurational fluctuations. This dynamical transition can be considered as a precursor of the collapse transition, characterized by the complete unfolding of the protein and associated to the crossing of the free energy barrier at ST3 in Fig. 2(a).

As a matter of fact just above T_θ an *almost* linear regime is observable in a narrow temperature interval, namely $0.68 \leq T \leq 0.80$, we believe that this further linear regime is due to fluctuations of the dihedral angles entering in the potential term V_3 . We found that, in this temperature range the linear increase is characterized by a slope $(\gamma_1 + \gamma_2 + \gamma_3) \sim 2.24$, leading to an estimate for the new contribution $\gamma_3 \sim 2.07$ which is of the order of $3/D_i = 2.5$ (by assuming that no neutral bead

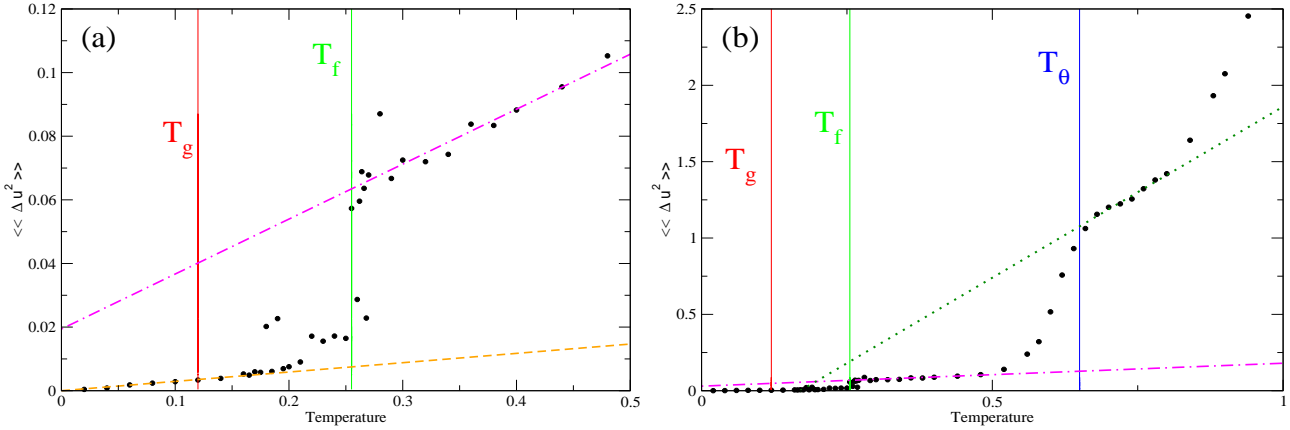


Fig. 4. (Color online) Variance $\langle\langle\Delta u^2\rangle\rangle$ versus temperature T , as estimated from equilibrium unfolding simulations of duration $t = 500,000$. The (black) dots are the results of the simulations, while in (a) the dashed (orange) line corresponds to $\langle\langle\Delta u^2\rangle\rangle = \gamma_1 T$ with $\gamma_1 = 0.02935$ and the dash-dotted (magenta) line to $\langle\langle\Delta u^2\rangle\rangle = (\gamma_1 + \gamma_2)T + d_0$ with $\gamma_2 = 0.1434$. In (b) the dotted (green) line refers to $\langle\langle\Delta u^2\rangle\rangle = (\gamma_1 + \gamma_2 + \gamma_3)T + d_1$ with $\gamma_3 = 2.067$.

is involved in the oscillating dihedral angles). These fluctuations are indeed more collective since they involve four consecutive beads. A third dynamical transition appears to take place around $T_{D3} \sim 0.82$. This latter transition is probably related to fluctuations involving large part of the protein.

Therefore each of the observed dynamical transitions is first characterized by small oscillations around some *typical equilibrium configuration* (this corresponds to the linear regime) followed by larger fluctuation induced by the breaking of hydrophobic bonds and leading to a new *equilibrium configuration* of the protein (this phase is characterized by an abrupt increase in the protein fluctuations). Once the protein is rearranged one observes another linear regime due to the activation of a different set of degrees of freedom, which were previously hindered by the hydrophobic interactions. At temperatures $T \leq T_{D1}$ the protein stays essentially in tightly packed native-like configuration and the only allowed oscillations are those of the beads around their equilibrium positions. At $T_f < T \leq T_{D2}$ the protein visits a different sets of less packed equilibrium configurations of the free energy, which are still characterized by a native core essentially intact. In this regime the bending oscillations of three consecutive beads become possible and are present together with harmonic oscillations of each bead. The transition at T_θ leads essentially to configurations almost completely stretched where fluctuations involving four consecutive beads (defining a dihedral angle) are now also activated.

From the analysis of $\langle\langle\Delta u^2\rangle\rangle$ we have no indication of the glassy transition occurring at T_g , apart some fluctuation taking place just above T_g as shown in Fig. 4(a). This is probably due to the fact that we have traced the dynamics of the protein for too short time windows. However, by increasing by a factor five the integration time, we do not observe substantial modifications in the behavior of $\langle\langle\Delta u^2\rangle\rangle$.

§7. Conclusions

In the present paper, we have discussed how the FEL of a model protein driven out of equilibrium can be estimated by exploiting two different methods: namely, we applied a work fluctuation relation and the IS approach. The results obtained with the two methods compare well, although the IS approach provides a reliable estimate of the FEL already at larger pulling velocities compared to the first method.

The FEL reveals three structural transitions along the unfolding pathways. By evaluating the potential energy landscape, we are able to assign a characteristic temperature to each of these structural transitions. Such temperatures compare well with the temperatures characterizing the *thermal* (un)folding of the molecule. Finally we analyze in detail the equilibrium structure fluctuations which mark the folding and collapse thermal transitions. Inspection of these fluctuations' variance allows us to identify the dynamical transitions which turn out to be precursors of the two corresponding structural transitions (namely, ST2 and ST3).

In conclusion, our work provides strong evidence that, at least for the present protein model, the mechanical out-of-equilibrium unfolding pathways can be reconciled with the thermal folding and unfolding ones, provided that one performs a detailed analysis of the relevant quantities, namely the free and potential energy landscapes, and the thermal transition temperatures.

Acknowledgements

We would like to thank S. Lepri for useful suggestions and discussions. This work has been partially supported by the Italian project "Dinamiche cooperative in strutture quasi uni-dimensionali" N. 827 within the CNR programme "Ricerca spontanea a tema libero". AI gratefully acknowledges support for computing resources from Danish Centre for Scientific Computing (DCSC).

References

- 1) J.R. Forman and J. Clarke, *Curr. Opin. Struct. Biol.* **17** (2007), 58.
- 2) B. Onoa B *et al*, *Science* **299** (2003) 1892.
- 3) D. Collin *et al*, *Nature* **437** (2005) 231.
- 4) C. Jarzynski, *Phys. Rev. Lett.* **78** (1997) 2690; C. Jarzynski, *Phys. Rev. E* **56** (1997) 5018; G.E. Crooks, *J. Stat. Phys.* **90** (1998) 1481; G.E. Crooks, *Phys. Rev. E* **60** (1999) 2721.
- 5) G. Hummer and A. Szabo, *Proc. Natl. Acad. Sci. USA.* **98** (2001) 3658.
- 6) A. Imparato, A. Pelizzola, and M. Zamparo, *Phys. Rev. Lett.* **98** (2007) 148102; A. Imparato, A. Pelizzola, M. Zamparo, *J. Chem. Phys.* **127** (2007) 145105.
- 7) A. Imparato, S. Luccioli, and A. Torcini, *Phys. Rev. Lett.* **99** (2007), 168101; S. Luccioli, A. Imparato, and A. Torcini, *Phys. Rev. E* **78** (2008), 031907.
- 8) S. Mitternacht, S. Luccioli, A. Torcini, A. Imparato, A. Irbäck, *Biophys. J.* **96** (2009) 429.
- 9) N. C. Harris, Y. Song, and C.-H. Kiang, *Phys. Rev. Lett.* **99** (2007) 068101.
- 10) A. Imparato, F. Sbrana, and M. Vassalli, *Europhys. Lett.* **82** (2008) 58006.
- 11) S. Sastry, P. G. Debenedetti, and F. H. Stillinger, *Nature (London)* **393** (1998) 554.
- 12) L. Angelani, R. Di Leonardo, G. Ruocco, A. Scala, and F. Sciortino, *Phys. Rev. Lett.* **85** (2000) 5356.
- 13) J.D. Honeycutt and D. Thirumalai, *Proc. Natl. Acad. Sci. U.S.A.* **87** (1990) 3526.
- 14) R.S. Berry, N. Elmaci, J.P. Rose, and B. Vekhter, *Proc. Natl. Acad. Sci. U.S.A.* **94** (1997) 9520.

- 15) T. Veitshans, D. Klimov, and D. Thirumalai, *Folding & Design* **2** (1997) 1.
- 16) A. Rampioni, *Caratterizzazione del panorama energetico di piccoli peptidi al variare della loro lunghezza*, PhD Thesis (Firenze, 2005)
- 17) J. Kim and T. Keyes, *J. Phys. Chem. B* **111** (2007) 2647
- 18) Z. Guo and D. Thirumalai, *Biopolymers*, **36** (1995) 83.
- 19) Z. Guo and C.L. Brooks III, *Biopolymers*, **42** (1997) 745-757.
- 20) D.A. Evans and D.J. Wales, *J. Chem. Phys* **118** (2003) 3891.
- 21) J. Kim, J.E. Straub, and T. Keyes, *Phys. Rev. Lett.* **97** (2006), 050601.
- 22) D.J. Lacks, *Biophys. J.* **88** (2005) 3494.
- 23) F.-Y. Li, J.-M. Yuan, and C.-Y. Mou, *Phys. Rev. E* **63** (2001), 021905.
- 24) A. Imparato, L. Peliti, *J. Stat. Mech.* (2006) P03005.
- 25) D.J. Wales, *Energy Landscapes*, Cambridge University Press, Cambridge, 2003.
- 26) F.H. Stillinger and T.A. Weber, *Science* **225** (1984) 983.
- 27) N. Nakagawa and M. Peyrard, *Proc. Natl. Acad. Sci. USA* **103** (2006) 5279; *Phys. Rev. E* **74** (2006), 041916.
- 28) A. Torcini *et al.* *J. Biol. Phys.* **27** (2001) 181; L. Bongini *et al.* *Phys. Rev. E* **68** (2003), 061111.
- 29) D.A. Evans and D.J. Wales, *J. Chem. Phys* **121** (2004) 1080.
- 30) W. Doster, *Eur. Biophys. J.* **37** (2008), 591
- 31) D.J. Bicout and G. Zaccai, *Biophys. J.* **80** (2001), 1115
- 32) F.G. Parak, *Curr. Opin. Struct. Biol.* **13** (2003), 552